Synthesis, Structures, and Properties of a Series of $[Cd_8Se(SePh)_{12}Cl_4]^{2-}$ Cluster Compounds with Different Counterions

Andreas Eichhöfer,*[a] Oliver Hampe,[a] and Martine Blom[a]

Keywords: Cluster compounds / Cadmium / Selenium / X-ray diffraction / UV/Vis spectroscopy / Mass spectrometry

A series of seven single-crystalline ionic CdSe cluster compounds, all possessing the cluster anion $[Cd_8Se(SePh)_{12}Cl_4]^{2-}$, but with different counterions, has been synthesized. The compounds were characterized in the solid state, solution, and gas phases using single-crystal XRD, powder XRD, UV/Vis spectroscopy, and FT mass spectrometry. The results of the crystal structure determination show that the increasing size of the different counterions does not simply lead to an increase in the shortest inter-cluster distance, but rather to changes in the crystal structure. Room-temperature UV/Vis absorption and reflectance spectra of the crystalline powders are virtually identical, proving that the electronic transitions in the energy range probed can be attributed to the cluster anion $[Cd_8Se(SePh)_{12}Cl_4]^{2-}$. The band of the first transition in the solid-state UV/Vis spectra are broadened relative to that in the solution spectra, as it is possibly affected by the collective interactions between the nanoclusters in the three-dimensional crystal lattice. Interestingly, in solution, the position and feature of the lowest-energy transition band changes as the solvent is varied. As FT mass spectrometry gives clear evidence for the existence of the intact $[Cd_8Se(SePh)_{12}Cl_4]^{2-}$ cluster anion in all these solutions, these shifts can be interpreted in terms of solvatochromic effects.

Introduction

Recent progress in the syntheses of CdSe cluster molecules has led to the development of a series of homologous compounds, namely $[NPr_4^+]_2[Cd_4(SePh)_6Cl_4]^{2-}$ $[Cd_{10}Se_4(SePh)_{12}(PPr_3)_4]$, $[Cd_{17}Se_4(SePh)_{24}(PPh_2Pr)_4]^{2+}[Cd_8Se(SePh)_{12}Cl_4]^{2-}$, and $[Cd_{32}Se_{14}(SePh)_{36}(PPh_3)_4]$ (Ph = phenyl, Pr = *n*-propyl).[1] As the largest clusters already overlap in size with the smallest nanocrystals, these clusters of semiconductor materials, composed of tens of atoms with bonding resembling that present in the solid state, are interesting molecular models for the investigation of the evolution of properties with size.[2−4] Systematic studies of the size-dependent optical and electronic properties of the CdSe cluster molecules mentioned above show that the onset of the absorption and low-temperature photoluminescence excitation of the clusters systematically shift to the blue in smaller clusters, manifesting the quantum confinement effect well known for larger CdSe nanocrystals. Photo-darkening experiments on the ionic cluster $[Cd_{17}Se_4(SePh)_{24}(PPh_2Pr)_4]^{2+}[Cd_8Se(SePh)_{12}Cl_4]^{2-}$ provide the first evidence for collective interactions between the cluster molecules within the crystalline solids. The results from a recent report by Döllefeld et al. on the absorption and reflectance spectra of $[Cd_{17}S_4(SCH_2CH_2OH)_{26}]$ cluster molecules show that collective interactions in the crystalline state also influence the lowest energy transition bands relative to the those in solution.[5,6]

In the work presented herein, we study the influence of the subsequent change in the type of counterion used in the synthesis of the cluster anion $[Cd_8Se(SePh)_{12}Cl_4]^{2-}$ on the properties of the compounds formed in solution and in the solid state. The compounds were characterised using X-ray diffraction on single crystals and crystalline powders, as well as by using different spectroscopic methods such as UV/Vis spectroscopy and electrospray Fourier transform mass spectrometry. The latter has proven to be a powerful tool in identifying charged, large cluster species present in solution.[7]

Results and Discussion

Cluster compounds **1**−**7** have been synthesised according to Scheme 1. Different conditions were optimised for the crystallisation of the different clusters, depending on the type of counterion present.

Structure Determination by Single-Crystal X-ray Diffraction

For all the compounds, crystal structures have been determined by single-crystal X-ray analysis. The molecular structure of the cluster anion $[Cd_8Se(SePh)_{12}Cl_4]^{2-}$ is similar for all the compounds studied (Figure 1).[8,9] A central selenium atom Se1 is tetrahedrally surrounded by four "in-

[a] Institut für Nanotechnologie, Forschungszentrum Karlsruhe, Postfach 3640, 76021 Karlsruhe, Germany
Fax: (internat.) + 49-7247/82-6368
E-mail: eichhoefer@int.fzk.de

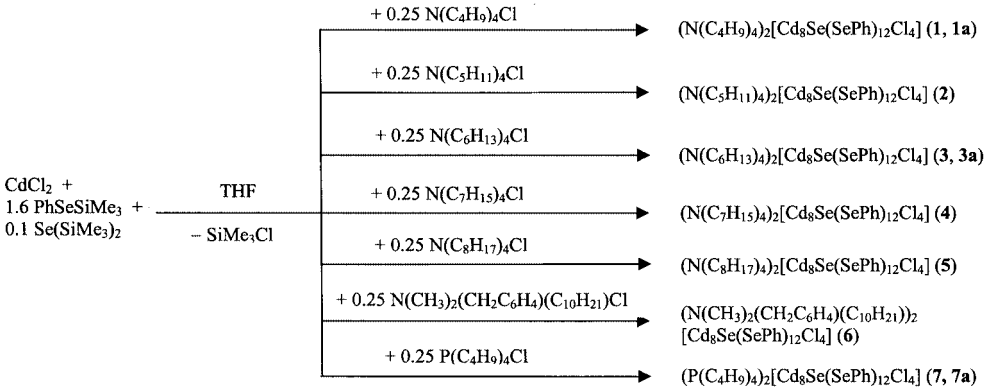

Scheme 1

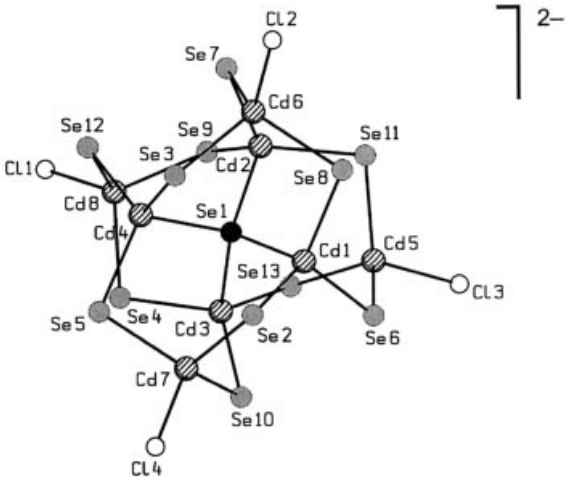

Figure 1. Molecular structure of the cluster anion $[Cd_8Se(SePh)_{12}Cl_4]^{2-}$ in **1**–**7**; C and H atoms are omitted for clarity; Se^{2-}: black, μ_2-$SePh^-$: grey, Cd^{2+}: hatched, and Cl^-: open circles

ner" cadmium atoms Cd1 to Cd4. Each of these four inner cadmium atoms is bound, through three μ_2-$SePh^-$ ligands (Se2 to Se13), to one of the four "outer" cadmium atoms Cd5 to Cd8, which also form a tetrahedron. In addition, each of the four outer cadmium atoms is bound to a terminal chloro ligand (Cl1 to Cl4). Each of the eight cadmium atoms has a distorted tetrahedral coordination sphere. The selenium atoms form a distorted icosahedron with the eight cadmium atoms bridging the triangular faces, whereby four of the cadmium atoms lie within, and four outside the icosahedron. The ranges of selected bond lengths are listed in Table 1 and display similar values for **1**–**7**, with the exception of the Cd–Se1 bond length range in **6**. In this compound a THF molecule is located close to Cd1 (Cd1–O2 2.813 Å), which possibly elongates the Cd1–Se1 bond length to a value of 2.672 Å.

The main difference in the structures of **1**–**7** arises as a result of the different crystal packing of the cluster anions and the ammonium or phosphonium cations. An interesting feature is the variation in the cluster–cluster distance in the crystal lattice. In Table 1, the variation of the shortest inter-cluster distances, measured as the distance between the central selenium atoms of the molecules, is shown (**1**: 15.076 Å, **1a**: 14.741 Å, **2**: 15.160 Å, **3**: 14.238 Å, **3a**: 14.995, **4**: 15.320 Å, **5**: 14.086 Å, **6**: 13.947 Å, **7**: 14.020 Å, **7a**: 14.145 Å). For all cluster molecules, the shortest inter-cluster distance varies from 13.95 Å in **6** to 15.32 Å in **4**. The trend in the variation of these distances is also followed by the shortest inter-cluster interactions between the selenium atoms. Interestingly, these values do not show a systematic increase with increasing length of the alkyl chain of the ammonium counterion. Even in **2**, **3a**, and **4**, which crystallise in the same space group with similar packing of the cluster molecules, inter-cluster distances do not systematically increase. In addition, different values for the pairs of similar compounds **1**, **1a** and **3**, **3a** and **7**, **7a** show that the size of the counterion is not the only parameter influencing the inter-cluster distance. The flexibility of the alkyl chains

Table 1. Selected ranges of bond lengths for **1**–**7a** including inter-cluster distances

	1	**1a**	**2**	**3**	**3a**	**4**	**5**	**6**	**7**	**7a**
Se1–Cd [Å]	2.616–2.630(2)	2.604–2.627(2)	2.613–2.622(1)	2.603–2.621(1)	2.612–2.625(2)	2.610–2.620(1)	2.608–2.628(2)	2.619–2.672(1)	2.612–2.627(1)	2.610–2.619(1)
μ_2-PhSe–Cd [Å]	2.627–2.691(2)	2.621–2.681(2)	2.629–2.696(2)	2.621–2.682(1)	2.617–2.678(2)	2.617–2.691(1)	2.617–2.681(1)	2.622–2.677(1)	2.629–2.701(2)	2.630–2.683(1)
Cl–Cd [Å]	2.432–2.448(5)	2.443–2.451(3)	2.425–2.445(3)	2.421–2.460(3)	2.416–2.447(3)	2.422–2.447(2)	2.426–2.458(4)	2.444–2.460(2)	2.434–2.445(3)	2.443–2.444(2)
Shortest inter-cluster distances [Å][a]	15.076	14.741	15.160	14.238	14.995	15.320	14.086	13.947	14.020	14.145

[a] Inter-cluster distances were measured as the distances between the central selenium atoms of the cluster molecules.

allows for the variable arrangements of the cations in the space between the $[Cd_8Se(SePh)_{12}Cl_4]^{2-}$ cluster anions, which, in addition to the incorporation of a varying number of solvent molecules, leads to the formation of different crystal packings. We found that the crystals incorporate more solvent molecules with increasing length of the alkyl chain of the ammonium cations, and as a result the crystal decomposes faster when separated from the mother liquor. Cations with more rigid and more bulky organic ligands than the "structurally weak" alkyl groups used here could lead to a better spacing of the cluster ions.

Powder X-ray Diffraction

In order to check the purity of the samples with respect to the possibility of the crystallisation of mixtures of different crystalline cluster compounds, as observed for **3**, **3a** and **7**, **7a**, powder X-ray diffraction patterns were measured for all compounds and compared with the calculated peak patterns from the data of the corresponding single-crystal X-ray analysis. The diffraction pattern of **4** (Figure 2, top) displays a good agreement between theory and experiment, however, those for **1**, **1a**, **2**, **3**, **3a**, **5**, **6**, **7**, and **7a** do not match the calculated patterns. Although the powder patterns show intense peaks in the low-angle region, the position of the peaks does not fit and the patterns could not be indexed. However, elemental analyses, UV/Vis spectra, and FT mass spectra (see below) all indicate the existence of the clusters determined by single-crystal X-ray diffraction. The powder patterns display no phase change on cooling from room temperature to 200 K. Determinations of the cell parameters of the single crystals at different temperatures also do not support the occurrence of phase changes, although difficulties do arise from the easy decomposition of the crystals at higher temperatures as a result of the loss of solvent molecules. Therefore, we suggest that the diffraction patterns of the dried crystalline powders show that the cluster molecules still present an order, but with a slight change in the lattice due to the loss of solvent molecules during the drying of the powder samples. In good agreement with this suggestion is the fact that the diffraction patterns of the crystalline powders in the mother liquor perfectly fit those calculated. The change in the curves by subsequent drying of the crystalline powder of **6** is shown in Figure 2 (bottom). The powder patterns of **3**, **3a** and **7**, **7a** measured in this way display peaks of both crystallographic species.

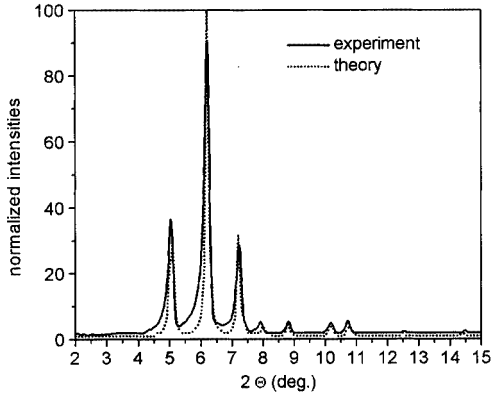

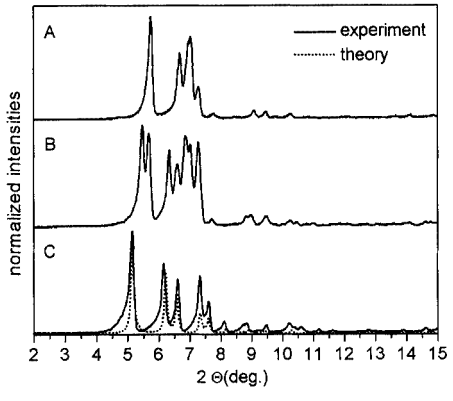

Figure 2. Top: room-temperature powder diffraction patterns of the dried crystalline powders of $[N(C_7H_{15})_4]_2[Cd_8Se(SePh)_{12}Cl_4]$ (**4**); bottom: change in room-temperature powder diffraction pattern of $[N(CH_3)_2(CH_2C_6H_4)(C_{10}H_{21})]_2[Cd_8Se(SePh)_{12}Cl_4]$ (**6**) by subsequent drying; A: dried under vacuum (10^{-3} bar); B: dried under nitrogen flow; C: as a suspension in THF (theoretical curve shown as dotted line)

FT Mass Spectrometry

Figure 3 shows a negative ion mass spectrum obtained by spraying a solution of crystalline **1** in 1,2-dichloroethane at a cone voltage of 25 V. It shows four peaks A−D that we identify as double negatively charged species: $[Cd_8Se(SePh)_{11}Cl_5]^{2-}$, $[Cd_8Se(SePh)_{12}Cl_4]^{2-}$, $[Cd_8Se(SePh)_{13}Cl_3]^{2-}$, $[Cd_8Se(SePh)_{14}Cl_2]^{2-}$, respectively. The inset compares the high-resolution mass spectrum of peak B with the simulated isotope distribution pattern of $[Cd_8Se(SePh)_{12}Cl_4]^{2-}$.

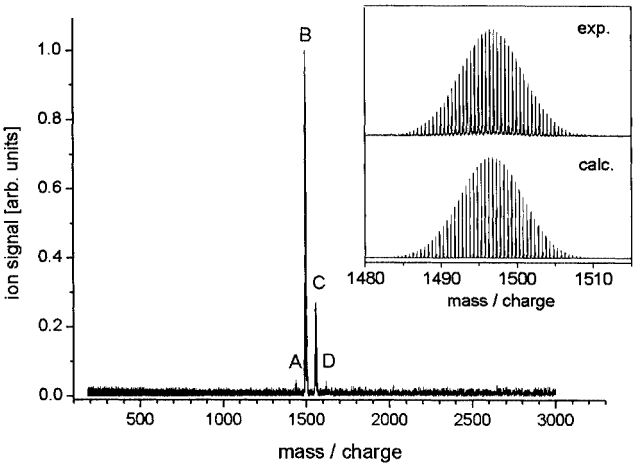

Figure 3. Electrospray FT mass spectrum of $[N(C_4H_9)_4^+]_2[Cd_8Se(SePh)_{12}Cl_4]^{2-}$ (**1**) in negative ion mode; the inset shows the high-resolution peak B ($[Cd_8Se(SePh)_{12}Cl_4]^{2-}$), experiment and simulation

Table 2. Assignment of the observed negative ions in the ESI mass spectra (as shown in Figure 3)

Peak	Ion	*m/z* (exp.)	*m/z* (calcd.)	Rel. intensity
A	$[Cd_8Se(SePh)_{11}Cl_5]^{2-}$	1436.41	1436.24	0.04
B	$[Cd_8Se(SePh)_{12}Cl_4]^{2-}$	1496.41	1496.55	1.00
C	$[Cd_8Se(SePh)_{13}Cl_3]^{2-}$	1556.92	1556.87	0.25
D	$[Cd_8Se(SePh)_{14}Cl_2]^{2-}$	1616.93	1617.18	0.03

The results are summarised in Table 2. It is worth noting that no fragmentation of the cluster ion occurred as long as cone voltages were kept below 30 V. This proves the high stability of these cluster complexes and also strongly suggests that these species are present intact in solution. Mass spectra taken from all seven compounds **1**−**7**, under virtually identical conditions, reveal very similar results, with slight variations in the relative intensities of peaks A−D. The observation of peaks A, C, and D next to the parent ion B is indicative of a ligand exchange process. Ligand exchange reactions were recently observed in electrospray mass spectrometric studies on thiophenolate-capped clusters of CdS, CdSe, and ZnS,[10−12] under conditions where partial fragmentation also takes place. Contrary to these studies, the mass spectra of our selenophenolate-bridged clusters do not show any ion signal due to Cl^- or $SePh^-$.

Given the relative ion intensities observed, the cluster has a tendency to lose Cl^- in favour of $SePh^-$, while keeping the total number of ligands constant. This could indicate that the cluster keeps its original structure as shown in Figure 1. This exchange can be attributed to the fact that $SePh^-$ is a better bridging ligand than Cl^-. However, the observation of $[Cd_8Se(SePh)_{11}Cl_5]^{2-}$ proves that a bridging $SePh^-$ ligand which is replaced by Cl^- potentially leads to a species with halide bridging. As the FT mass spectra show the same peaks when using different solvents, namely THF, acetonitrile, dichloromethane, and 1,2-dichloroethane, we deduce that this ligand exchange is a direct result of intercluster reactions.

Warming and cooling of the solutions of the cluster molecules do not lead to a change in the observed mass spectra or UV/Vis spectra (see next chapter). Mass spectra taken from solutions after one week also do not differ from the original spectra, showing their intrinsic stability.

UV/Vis Spectroscopy

UV/Vis absorption spectra of solutions of **1**−**7** in 1,2-dichloroethane were measured. All compounds display a very similar spectrum, with a maximum at 301 nm and a minimum at 284 nm. Figure 4 shows the absorption spectra of **2** with $\varepsilon = 6.12 \cdot 10^4\ M^{-1}cm^{-1}$ at 301 nm (dashed line). According to these results, it is obvious that the different counterions have virtually no effect on the absorption behaviour of the cluster anions in solution. Solid state reflectance spectra of **1**−**7** were measured directly on the milled crystalline powders or as a mull in oil between two quartz plates inside an integrating sphere (Figure 4). For all compounds, the onset of the absorption shifts slightly to

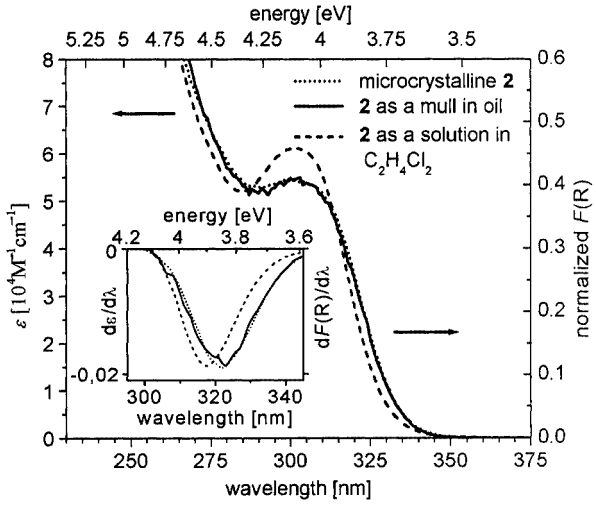

Figure 4. UV/Vis absorption spectrum of $[N(C_5H_{11})_4]_2[Cd_8Se(SePh)_{12}Cl_4]$ (**2**) in $C_2H_4Cl_2$ (dashed line) and UV/Vis reflectance spectra of **2** as a mull in mineral oil (straight line) and as a microcrystalline powder (dotted line); the inset shows part of the first derivative spectra

lower energies relative to that in the solution spectra. This is accompanied by a loss of structure, as can be seen from the spectra of **2** in Figure 4. Slight differences in the solid state spectra of **1**−**7** are thought to arise mostly from the quality of the mull, since the concentration and grain sizes cannot be kept constant for all the samples. Therefore, these differences cannot be related to the different spacing of the $[Cd_8Se(SePh)_{12}Cl_4]^{2-}$ cluster anions in the crystal lattice. Further, the powder X-ray diffraction patterns reveal that the crystals lose solvent molecules on drying, which is accompanied by a change in the packing in the crystal lattice. This leads to the deduction that the different counterions have no distinct influence on the UV/Vis absorption spectra of the $[Cd_8Se(SePh)_{12}Cl_4]^{2-}$ cluster anion in the solid state as well.

The broadening of the solid state spectra, indicated by a shift of the maximum of the first derivative by about 55 meV to lower energies with respect to the spectra in solution, could result from the effect of the crystal packing and/or of the counterion on the electronic properties in the solid state, as was recently suggested by Döllefeld et al. for crystals of $[Cd_{17}S_4(SCH_2CH_2OH)_{26}]$.[5] They found a shift of the first electronic transition to lower energies by about 150 meV in the reflectance spectra of micron-sized crystals, relative to that in their solution spectra in DMF. They suggest that both the electronic and the dipole−dipole interactions play a role in the complete description of the interactions between semiconductor nanoclusters in crystalline superstructures. Besides the difference in charges, the main difference between the compound $[Cd_{17}S_4(SCH_2CH_2OH)_{26}]$ investigated by Döllefeld et al. and the $[Cd_8Se(SePh)_{12}Cl_4]^{2-}$ cluster anions in this work is the fact that the former are directly bonded in the crystal lattice to one another by bridging thiolato ligands. The remarkable change in the solid state and solution spectra in this case may arise from

the breaking of the covalent bonds of the bridging thiolato groups by the strongly coordinating solvent DMF. This suggestion is also supported by the fact that the authors can find for thin layers of this cluster deposited from DMF solutions only a broadening of the lowest energy transition in comparison to the spectra of the DMF solutions.[6]

Regarding the $[Cd_8Se(SePh)_{12}Cl_4]^{2-}$ cluster anions, the use of various solvents, with a range of dielectric constants (ε_r), has a clear effect on the absorption properties of the cluster molecules, as can be seen for **7**, **7a** (Figure 5). The absorption spectra in dichloromethane (ε_r = 8.9) and 1,2-dichloroethane (ε_r = 10.2) are very similar, whereas the first absorption maximum in acetonitrile (ε_r = 37.5) is shifted by about 41 meV to a higher energy. The shape of the first absorption peak in the spectra of **7**, **7a** in THF (ε_r = 7.6) is more featureless and broader than those in the other solution spectra. While the value for the first absorption maximum is similar to that found in acetonitrile, the inflection point (maximum of the first derivative) is similar to that in the two chlorinated solvents. Therefore, the shift of the lowest energy absorption band does not simply follow the change in the permittivity of the medium, but is probably more affected by the different coordination properties of the various solvents. In this context, it can be seen that a THF molecule coordinates one cadmium atom of the $[Cd_8Se(SePh)_{12}Cl_4]^{2-}$ cluster anion in **6**, leading to a coordination number of five for this metal atom.

FT mass spectrometry clearly shows the existence of the intact $[Cd_8Se(SePh)_{12}Cl_4]^{2-}$ cluster anion in all solutions. However, the observed ligand exchange reaction of chlorine atoms for phenylselenolato ligands could also have an effect on the UV/Vis absorption spectra, although we cannot rule out that these reactions take place in the electrospraying step. Interestingly, the use of the different solvents, THF, acetonitrile, dichloromethane, and 1,2-dichloroethane, leads to virtually identical products of ligand exchange, with slightly varying intensities in the FT mass spectra.

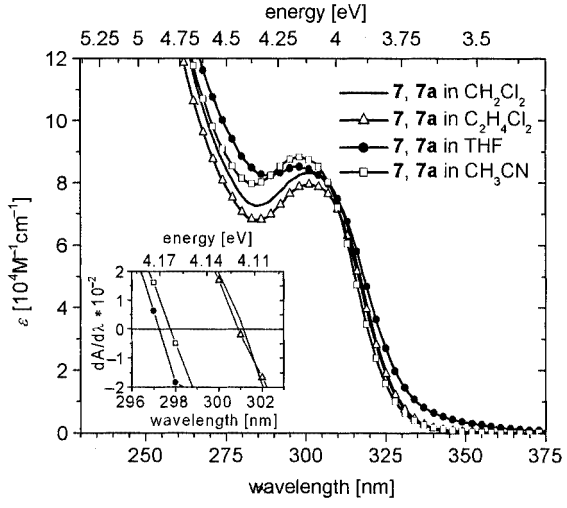

Figure 5. UV/Vis absorption spectra of $[P(C_4H_9)_4]_2[Cd_8Se(SePh)_{12}Cl_4]$ (**7**, **7a**) dissolved in different solvents; the inset shows part of the first derivative spectra; values for the relative dielectric constants, ε_r, of the solvents are: 8.9 (CH_2Cl_2), 10.2 ($C_2H_4Cl_2$), 7.6 (THF), 37.5 (CH_3CN)

Conclusions

A series of seven single-crystalline CdSe cluster molecules with the same $[Cd_8Se(SePh)_{12}Cl_4]^{2-}$ cluster anion has been synthesised by altering the counterion. The cluster molecules were characterised by a detailed analytical investigation, which included single-crystal XRD, powder XRD, UV/Vis spectroscopy, as well as FT mass spectrometry. The results of the crystal structure determination show that the increasing size of the different counterions does not simply lead to an increase in the shortest inter-cluster distances, but rather to changes in the crystal structure. Room-temperature UV/Vis absorption and reflectance spectra of the crystalline powders are virtually identical, proving that the electronic transitions in the energy range probed can be attributed to the cluster anion $[Cd_8Se(SePh)_{12}Cl_4]^{2-}$. The band of the lowest energy transition in the solid-state UV/Vis spectra are broadened relative to that in the solution spectra, as it is possibly affected by the collective interactions between the nanoclusters in the three-dimensional crystal lattice. Interestingly, in solution, the position and feature of the lowest energy transition band changes as the solvent is varied. As FT mass spectrometry gives clear evidence for the existence of the intact $[Cd_8Se(SePh)_{12}Cl_4]^{2-}$ cluster anion in all these solutions, these shifts can be interpreted in terms of solvatochromic effects.

Further studies will focus on the use of other counterions, including higher charged species and more rigid organic ligands, and on the crystallisation of larger ionic cluster molecules that are shown to be stable from simple theoretical calculations.[13] Additional synthetic interest arises from the possibility to form covalently linked two- or three-dimensional networks of these cluster molecules, through reaction of the four reactive Cd−Cl bonds with bifunctional silylated chalcogen compounds, such as $(Me_3Si)Se-R-Se(SiMe_3)$, where R = C_2H_4, C_3H_6, C_4H_8. Interesting collective phenomena based on direct cluster−cluster interactions are to be expected in these compounds.

Experimental Section

Syntheses: Standard Schlenk techniques were employed throughout the syntheses using a double manifold vacuum line with high-purity dry nitrogen. The solvents tetrahydrofuran and diethyl ether were dried with sodium/benzophenone and distilled under nitrogen. Anhydrous $CdCl_2$, as well as ammonium and phosphonium salts, were purchased from Aldrich. $PhSeSiMe_3$ [14] and $Se(SiMe_3)_2$ [15] were prepared according to standard literature procedures.

$[N(n\text{-}C_4H_9)_4]_2[Cd_8Se(SePh)_{12}Cl_4]$ (1, 1a): $CdCl_2$ (0.20 g, 1.09 mmol) and $N(n\text{-}C_4H_9)_4Cl$ (0.08 g, 0.27 mmol) were suspended in 130 mL of THF. $PhSeSiMe_3$ (0.33 mL, 1.74 mmol) was then added, and the resulting clear solution stirred overnight. Addition of $Se(SiMe_3)_2$ (0.025 mL, 0.11 mmol) at −40 °C, and warming to room temper-

ature led to the formation of colourless hexagonal plates of **1**, **1a**, with a total yield of 60% after further concentration of the solution. $C_{104}H_{132}Cd_8Cl_4N_2Se_{13}$ (3477.48): calcd. C 35.92, H 3.83, N 0.83; found C 35.93, H 3.98, N 0.88. Suitable crystals for single-crystal XRD were obtained either by layering the concentrated filtered solution with diethyl ether to yield **1**, or by recrystallising the white crystalline powder from THF at −20 °C to give **1a**.

$[N(n\text{-}C_5H_{11})_4]_2[Cd_8Se(SePh)_{12}Cl_4]$ (2): $CdCl_2$ (0.24 g, 1.31 mmol) and $N(n\text{-}C_5H_{11})_4Cl$ (0.11 g, 0.33 mmol) were suspended in 70 mL of THF. $PhSeSiMe_3$ (0.40 mL, 2.10 mmol) was then added, and the resulting clear solution was stirred overnight. Addition of $Se(SiMe_3)_2$ (0.029 mL, 0.13 mmol) at −30 °C, and warming to room temperature led to the formation of colourless crystals of **2** with a yield of 74%. **2** can be recrystallised from THF on careful addition of small aliquots of diethyl ether. $C_{112}H_{148}Cd_8Cl_4N_2Se_{13}$ (3589.99): calcd. C 37.47, H 4.16, N 0.78; found C 37.89, H 4.39, N 0.82.

$[N(n\text{-}C_6H_{13})_4]_2[Cd_8Se(SePh)_{12}Cl_4]$ (3, 3a): $CdCl_2$ (0.24 g, 1.31 mmol) and $N(n\text{-}C_6H_{13})_4Cl$ (0.13 g, 0.33 mmol) were suspended in 70 mL of THF. $PhSeSiMe_3$ (0.40 mL, 2.10 mmol) was then added, and the resulting clear solution stirred overnight. Addition of $Se(SiMe_3)_2$ (0.029 mL, 0.13 mmol) at −30 °C, and warming to room temperature led to the formation of colourless crystals of **3**, **3a**, with a yield of 62%. Suitable crystals of **3** were obtained directly from the reaction solution at room temperature, while crystals of **3a** were grown at 0 °C. $C_{120}H_{164}Cd_8Cl_4N_2Se_{13}$ (3702.21): calcd. C 38.93, H 4.46, N 0.76; found C 38.72, H 4.48; N 0.85.

$[N(n\text{-}C_7H_{15})_4]_2[Cd_8Se(SePh)_{12}Cl_4]$ (4): $CdCl_2$ (0.18 g, 0.98 mmol) and $N(n\text{-}C_7H_{15})_4Cl$ (0.11 g, 0.25 mmol) were suspended in 75 mL of THF. $PhSeSiMe_3$ (0.30 mL, 1.57 mmol) was then added, and the resulting clear solution stirred overnight. Addition of $Se(SiMe_3)_2$ (0.022 mL, 0.098 mmol) at −30 °C, and warming to room temperature led to the formation of a small amount of a precipitate of unknown composition. This was filtered, and on addition of 5 mL of diethyl ether, colourless crystals of **4** were formed with a 68% yield. **4** can be recrystallised from THF on addition of aliquots of diethyl ether. $C_{128}H_{180}Cd_8Cl_4N_2Se_{13}$ (3814.42): calcd. C 40.30, H 4.76, N 0.73; found C 38.98, H 4.76, N 0.63.

$[N(n\text{-}C_8H_{17})_4]_2[Cd_8Se(SePh)_{12}Cl_4]$ (5): $CdCl_2$ (0.21 g, 1.15 mmol) and $N(n\text{-}C_8H_{17})_4Cl$ (0.14 g, 0.25 mmol) were suspended in 50 mL of THF. $PhSeSiMe_3$ (0.35 mL, 1.84 mol) was then added, and the resulting clear solution stirred overnight. Addition of $Se(SiMe_3)_2$ (0.026 mL, 0.12 mmol) at −30 °C, and warming to room temperature led to the formation of a clear colourless solution. Concentration to 3 mL led to the formation of thin needles in a white precipitate of unknown composition. This was filtered, and on addition of 8 mL of diethyl ether, colourless crystals of **5** were formed with a 65% yield. **5** can be recrystallised from THF on addition of aliquots of diethyl ether. $C_{136}H_{196}Cd_8Cl_4N_2Se_{13}$ (3926.64): calcd. C 41.60, H 5.03, N 0.71; found C 41.08, H 4.99, N 0.75.

$[N(CH_3)_2(CH_2C_6H_4)(n\text{-}C_{10}H_{21})]_2[Cd_8Se(SePh)_{12}Cl_4]$ (6): $CdCl_2$ (0.17 g, 0.093 mmol) and $N(CH_3)_2(CH_2C_6H_4)(n\text{-}C_{10}H_{21})Cl$ (0.07 g, 0.23 mmol) were suspended in 60 mL of THF. $PhSeSiMe_3$ (0.28 mL, 1.49 mmol) was then added, and the resulting clear solution stirred overnight. Addition of $Se(SiMe_3)_2$ (0.021 mL, 0.093 mmol) at −30 °C, and warming to room temperature led to the formation of colourless crystals of **6**; concentration led to the further precipitation of crystals, yielding 71% of **6**. $C_{110}H_{128}Cd_8Cl_4N_2Se_{13}$ (3545.81): calcd. C 37.26, H 3.64, N 0.79; found C 38.61, H 4.02, N 0.94.

$[P(n\text{-}C_4H_9)_4]_2[Cd_8Se(SePh)_{12}Cl_4]$ (7, 7a): $CdCl_2$ (0.25 g, 1.36 mmol) and $P(n\text{-}C_4H_9)_4Cl$ (0.10 g, 0.34 mmol) were suspended in 150 mL of THF. $PhSeSiMe_3$ (0.42 mL, 2.18 mmol) was then added, and the resulting clear solution stirred overnight. Addition of $Se(SiMe_3)_2$ (0.031 mL, 0.14 mmol) at −30 °C, and warming to room temperature led to the formation of a colourless solution. Colourless crystals of **7**, **7a** were formed after concentration, with a 76% yield. Recrystallisation from THF/diethyl ether also yielded a mixture of crystals of **7** and **7a**. $C_{104}H_{132}Cd_8Cl_4P_2Se_{13}$ (3511.71): calcd. C 35.57, H 3.79 found C 35.58, H 3.94.

Structure Determinations: Crystals suitable for single-crystal X-ray diffraction were obtained directly from the reaction solutions of compounds **2**, **3**, **3a**, **4**, **6**, **7**, and **7a**. In the case of **1a** and **5**, crystals were grown by recrystallisation of the obtained microcrystalline powders. **1** was crystallised by layering of the concentrated reaction solution. Single-crystal X-ray diffraction data were collected using graphite-monochromatised Mo-K_α radiation (λ = 0.71073 Å) with a STOE IPDS (Imaging Plate Diffraction System), equipped with a SCHNEIDER rotating anode. All the structures were solved with the direct methods program SHELXS[16] of the SHELXTL PC suite programs, and they were refined with the use of the full-matrix least-squares program SHELXL.[16] Molecular diagrams were prepared using the program SCHAKAL 97.[17] All Cd, Se, and Cl atoms were refined with anisotropic displacement parameters. In **1a**, **3a**, **5**, **6**, **7**, and **7a**, the N, P, and the C atoms of the SePh rings were also refined anisotropically. The C atoms of the phenyl groups in **1** were refined isotropically as a rigid group. In **6**, the atoms C1 to C6, and in **3**, the atoms C55 to C60 are disordered. The C atoms of the ammonium and phosphonium counterions were all refined isotropically and show some disorder in the case of **3**, **6**, and **7**. In **5**, some of the C atoms of the $N(C_8H_{17})_4^+$ counterions show high thermal parameters due to the flexibility of the long alkyl chain and could only be refined with reduced occupancy. For one octyl chain in **5**, only four carbon atoms could be located in the difference fourier map. These problems probably arise from the fact that the crystals decompose, even at 110 K after 1 d of measurement. THF and Et_2O solvent molecules were mostly refined with half occupancy because of a high degree of disorder and large thermal parameters. The H atoms of the SePh groups were included in the calculated positions for **2**, **3a**, **4**, **7**, and **7a**. X-ray powder diffraction data (XRD) were collected with a STOE STADI P diffractometer (Cu-K_α radiation, germanium monochromator, Debye−Scherrer geometry). The measurements were performed on crystalline powders, dried or in mother liquor, in 0.5 mm sealed glass capillaries. Theoretical powder diffraction patterns for **1**−**7** were calculated on the basis of the atom coordinates obtained from single-crystal X-ray analysis using the program package STOE WinXPOW.[18] Crystal data for each compound are listed in Tables 3 and 4.[19]

UV/Vis Measurements: Absorption spectra of cluster molecules in solution were measured with a Perkin−Elmer Lambda 900 spectrophotometer in quartz cuvettes. Solid state reflectance spectra were measured with a Varian Cary 500 as micron-sized crystalline powders or as nujol mulls between quartz plates inside a Labsphere integrating sphere.

FT-Mass Spectrometry: Mass spectra were measured with a 7-Tesla-APEX II Fourier transform mass spectrometer (Bruker Daltonics) equipped with an electrospray ionisation source (Analytica of Branford). Freshly prepared solutions of compounds **1**−**7** in $C_2H_4Cl_2$ (ca. 0.1 mmol/L) were sprayed employing a syringe infusion pump (Cole-Parmer), at typical rates of 300 μL/h. Neat nitro-

Table 3. Crystallographic data for $[N(n\text{-}C_4H_9)_4]_2[Cd_8Se(SePh)_{12}Cl_4]$ (**1**, **1a**), $[N(n\text{-}C_5H_{11})_4]_2[Cd_8Se(SePh)_{12}Cl_4]$ (**2**), and $[N(n\text{-}C_6H_{13})_4]_2[Cd_8Se(SePh)_{12}Cl_4]$ (**3**, **3a**)

	1·0.5C_4H_8O	**1a**·5C_4H_8O	**2**·0.5C_4H_8O	**3**·0.5C_4H_8O	**3a**·2C_4H_8O
Formula mass [g/mol]	3513.65	3838.12	3622.83	3738.06	3846.22
Crystal system	triclinic	monoclinic	orthorhombic	monoclinic	orthorhombic
Space group	$P\bar{1}$	$P2_1/c$	$Pna2_1$	$P2_1/n$	$Pna2_1$
a [Å]	21.471(2)	19.543(4)	27.818(6)	21.510(4)	28.077(6)
b [Å]	26.694(5)	29.694(6)	22.156(4)	29.364(6)	21.500(4)
c [Å]	28.815(5)	32.266(7)	24.009(5)	24.494(5)	25.113(5)
α [°]	114.08(2)	90	90	90	90
β [°]	90.99(2)	103.09(3)	90	91.79(3)	90
γ [°]	90.04(2)	90	90	90	90
V [Å^3]	15076(4)	18238(6)	14798(5)	15463(5)	15160(5)
Z	4	4	4	4	4
T [K]	200	110	200	200	200
d_c [g·cm^{-3}]	1.548	1.398	1.626	1.606	1.685
μ(Mo-K_α) [mm^{-1}]	4.35	3.604	4.434	4.25	4.334
F[000]	6736	7456	6980	7248	7488
$2\theta_{max}$ [°]	50	52	50	50	50
Meas. reflns.	67932	96163	62906	73397	58768
Unique reflns.	45880	35341	23880	26235	24285
R_{int}	0.0863	0.1106	0.0627	0.0931	0.1095
Reflns. with $I > 2\sigma(I)$	25771	25515	19147	19591	20914
Refined params.	812	1220	703	776	1125
$R1$ [$I > 2\sigma(I)$][a]	0.0791	0.0883	0.0470	0.0705	0.0668
$wR2$ (all data)[b]	0.2976	0.2580	0.1368	0.2156	0.1920
Abs. structure parameter	–	–	0.201(8)	–	0.160(10)

[a] $R1 = \Sigma||F_o| - |F_c||/\Sigma|F_o|$. [b] $wR2 = \{\Sigma[w(F_o^2 - F_c^2)^2]/\Sigma[w(F_o^2)^2]\}^{1/2}$.

Table 4. Crystallographic data for $[N(n\text{-}C_7H_{15})_4]_2[Cd_8Se(SePh)_{12}Cl_4]$ (**4**), $[N(n\text{-}C_8H_{17})_4]_2[Cd_8Se(SePh)_{12}Cl_4]$ (**5**), $[N(CH_3)_2(CH_2C_6H_4)(n\text{-}C_{10}H_{21})]_2[Cd_8Se(SePh)_{12}Cl_4]$ (**6**), and $[P(n\text{-}C_4H_9)_4]_2[Cd_8Se(SePh)_{12}Cl_4]$ (**7**, **7a**)

	4·0.5C_4H_8O	**5**·2.25C_4H_8O·1.25$C_4H_{10}O$	**6**·1C_4H_8O	**7**·2C_4H_8O	**7a**·1.5C_4H_8O
Formula mass [g/mol]	3832.26	4217.36	3617.73	3655.72	3675.78
Crystal system	orthorhombic	triclinic	monoclinic	triclinic	monoclinic
Space group	$Pna2_1$	$P\bar{1}$	$P2_1/n$	$P\bar{1}$	$C2/c$
a [Å]	28.359(6)	26.221(5)	21.690(4)	16.984(3)	23.741(5)
b [Å]	22.153(4)	29.220(6)	28.180(6)	19.390(2)	25.649(5)
c [Å]	24.495(5)	31.148(6)	23.327(5)	26.151(5)	27.885(6)
α [°]	90	112.82(3)	90	100.417(18)	90
β [°]	90	97.12(3)	94.26(3)	93.81(2)	101.53(3)
γ [°]	90	113.43(3)	90	107.572(17)	90
V [Å^3]	15388(5)	19061(7)	14218(5)	8007(2)	16637(6)
Z	4	4	4	2	4
T [K]	200	110	200	200	200
d_c [g·cm^{-3}]	1.654	1.470	1.69	1.516	1.468
μ(Mo-K_α) [mm^{-1}]	4.269	3.455	4.615	4.117	3.964
F[000]	7468	8330	6944	3520	7088
$2\theta_{max}$ [°]	48	50	50	50	50
Meas reflns.	68066	63913	87029	83284	52866
Unique reflns.	23831	48059	24660	28015	13722
R_{int}	0.0459	0.0374	0.0581	0.1091	0.0751
Reflns. with $I > 2\sigma(I)$	19804	36989	18584	28015	11223
Refined params.	762	2531	760	1084	611
$R1$ [$I > 2\sigma(I)$][a]	0.0429	0.0570	0.0555	0.0726	0.0422
$wR2$ (all data)[b]	0.1246	0.1787	0.1949	0.2245	0.1662
Abs. structure parameter	0.027(8)	–	–	–	–

[a] $R1 = \Sigma||F_o| - |F_c||/\Sigma|F_o|$. [b] $wR2 = \{\Sigma[w(F_o^2 - F_c^2)^2]/\Sigma[w(F_o^2)^2]\}^{1/2}$.

gen was used as the spraying and drying gas, both kept at room temperature. Cone voltages were kept low enough to minimise fragmentation.

Acknowledgments

This work was supported by the German-Israel Fund, the Deutsch-Israelisches Programm (DIP) and the Forschungszentrum

Karlsruhe. A. E. wants to thank Dr. A. Eychmüller, Dr. M. Haase, and Dr. H. Döllefeld for helpful discussions concerning the measurement of the UV/Vis spectra of the solid samples, and Prof. Dr. H. Krautscheid for careful revision of the document. The authors are also grateful to E. Tröster for her invaluable assistance in the practical work.

[1] V. Soloviev, A. Eichhöfer, D. Fenske, U. Banin, *J. Am. Chem. Soc.* **2001**, *123*, 2354−2364.
[2] I. G. Dance, A. Choy, M. L. Scudder, *J. Am. Chem. Soc.* **1984**, *106*, 6285−6295.
[3] N. Herron, J. C. Calabrese, W. E. Farneth, Y. Wang, *Science* **1993**, *259*, 1426−1428.
[4] T. Vossmeyer, G. Reck, L. Katsikas, E. Haupt, B. Schulz, H. Weller, *Science* **1995**, *267*, 1476−1479.
[5] H. Döllefeld, H. Weller, A. Eychmüller, *Nanoletters* **2001**, *1*, 267−269.
[6] H. Döllefeld, H. Weller, A. Eychmüller, *J. Phys. Chem. B* **2002**, *106*, 5604−5608.
[7] D. Fenske, T. Langetepe, M. Kappes, O. Hampe, P. Weis, *Angew. Chem.* **2000**, *112*, 1925−1928; *Angew. Chem. Int. Ed.* **2000**, *39*, 1857−1860.
[8] G. S. H. Lee, K. J. Fisher, D. C. Craig, M. L. Scudder, I. G. Dance, *J. Am. Chem. Soc.* **1990**, *112*, 6435−6437.
[9] S. Behrens, D. Fenske, *Ber. Bunsenges. Phys. Chem.* **1997**, *101*, 1588−1592.
[10] J-J. Gaumet, G. F. Strouse, *J. Am. Soc. Mass Spectrom.* **2000**, *11*, 338−344.
[11] T. Løver, W. Henderson, G. A. Bowmaker, J. M. Seakins, R. P. Cooney, *Inorg. Chem.* **1997**, *36*, 3711−3723.
[12] T. Løver, G. A. Bowmaker, W. Henderson, R. P. Cooney, *Chem. Commun.* **1996**, *36*, 683−685.
[13] I. Dance, G. S. H. Lee, in: *The Chemistry of the Copper and Zinc Triads* (Eds.: A. J. Welch, S. K. Chapman), Royal Society of Chemistry, Cambridge, **1993**, p. 87.
[14] N. Miyoshi, H. Ishii, K. Kondo, S. Mui, N. Sonoda, *Synthesis* **1979**, 301−304.
[15] H. Schmidt, H. Ruf, *Z. Anorg. Allg. Chem.* **1963**, *321*, 270−273.
[16] G. M. Sheldrick, *SHELXTL, PC version 5.1, An Integrated System for Solving, Refining, and Displaying Crystal Structures from Diffraction Data*, Bruker Analytical X-ray Systems, Karlsruhe, **2000**.
[17] E. Keller, *SCHAKAL 97, A Computer Program for the Graphic Representation of Molecular and Crystallographic Models*, Universität Freiburg, **1997**.
[18] STOE, *WinXPOW*, STOE & Cie GmbH, Darmstadt, **2000**.
[19] CCDC-192112 to -192121 contain the supplementary crystallographic data for this paper. These data can be obtained free of charge at www.ccdc.cam.ac.uk/conts/retrieving.html [or from the Cambridge Crystallographic Data Centre, 12 Union Road, Cambridge CB2 1EZ, UK; Fax: (internat.) + 44-1223/336-033; E-mail: deposit@ccdc.cam.ac.uk].

Received August 22, 2002
[I02476]